

# Amyloid Filaments in Inclusion Body Myositis

## Novel Findings Provide Insight Into Nature of Filaments

Jerry R. Mendell, MD; Zarife Sahenk, MD; Tracy Gales, MS; Laura Paul

• **Inclusion body myositis (IBM)** represents a serious debilitating disease of muscle without identifiable cause or treatment. Muscle biopsy specimens have characteristic rimmed vacuoles, varying degrees of inflammation, and, most importantly, cytoplasmic and intranuclear filamentous inclusions of unknown composition. Fresh-frozen sections of muscle biopsy specimens from 24 IBM cases were stained with Congo red dye (pH, 10.5 to 11.0). Control biopsy specimens included polymyositis, dermatomyositis, hereditary vacuolar myopathies of unknown cause, acid maltase deficiency, distal myopathy, oculopharyngeal dystrophy, and chloroquine myopathy. Sections were also immunostained with antibody to transthyretin, human P component, and immunoglobulin light chains. In the vacuolated fibers in IBM, amyloidogenic green-birefringent deposits were seen. Some deposits were delicate and wispy appearing, and others were plaque-like. The size of deposits varied, measuring 1 × 2 to 8 µm, and rarely up to 20 µm in length. The number of amyloid-positive fibers correlated with the number of vacuolated fibers. Similar deposits were seen in one

case of distal myopathy and one hereditary vacuolar myopathy. Other control cases were negative for amyloid deposits. Antibody staining for known amyloidogenic proteins was negative. This study demonstrates that the filaments in IBM share properties with amyloid proteins. The location implies that this amyloid material is formed intracellularly, rather than having a systemic derivation. The association of amyloid deposits with autophagic vacuoles in IBM raises the likely possibility that the filaments represent a modification of a normal protein within an acidic degradative vacuolar compartment. An alternative possibility, considering the shared properties of IBM filaments and prions (which include size and amyloidogenic properties), is that IBM represents a human prion disease. Further studies will be required to resolve the nature of the amyloidogenic filaments in IBM, but these findings may provide clues to the pathogenesis of this poorly understood disorder. In addition, the findings should facilitate the clinical diagnosis of IBM.

(*Arch Neurol.* 1991;48:1229-1234)

use of electron microscopy, presents features of autophagia composed of whorls of membranous material and myelin figures, as well as amorphous debris.<sup>2,4</sup> In addition, endomysial inflammation occurs to varying degrees, characterized by focal invasion of non-necrotic muscle fibers by a 2:1 ratio of predominantly CD8+ cytotoxic/suppressor T cells to macrophages.<sup>6</sup> The definitive diagnosis of IBM rests on electron microscopic findings of filamentous inclusions.<sup>1,2,4</sup> The filaments are not membrane bound, but they often occur adjacent to the vacuoles. The diameter of the filaments has been reported to vary from 10 to 21 nm.<sup>1,4</sup>

The cause of IBM remains enigmatic. The significance of the filamentous inclusions represents a subject of debate. In 1967, Chou<sup>7</sup> described a myxovirus-like structure in a case of chronic polymyositis. In retrospect, this represented the first description of the filaments occurring in IBM. Subsequent work by Chou<sup>8</sup> emphasized that these inclusions reacted with antibodies raised against mumps virus antigens. This finding was not confirmed by other investigators<sup>9,10</sup> unable to demonstrate specific binding of anti-mumps antibodies in IBM.

The study presented herein provides new insight into the nature of IBM filaments. The findings strongly indicate that the filaments share histochemical properties with amyloid proteins, but the intracellular location distinguishes them from the more common types of systemic amyloid.<sup>11,12</sup> The close association of amyloidogenic filaments to autophagic vacuoles in IBM raises the possibility of accumulation of an altered protein. Alternatively, properties com-

The term *inclusion body myositis* (IBM) was coined in 1971 by Yunis and Samaha.<sup>1</sup> They described a disorder resembling polymyositis but distinctive because of the vacuolated muscle fibers and nuclear and cytoplasmic fibrillary inclusions. Controversy concerning the specificity of the histopathologic fea-

tures of inclusion body myositis delayed its general acceptance as a distinct disorder. Subsequent reports<sup>2,4</sup> have unequivocally established this as a well-defined entity. The disorder slightly predominates in male individuals and usually begins after age 50 years, although no age groups have been entirely excluded.<sup>3</sup> The diagnosis of IBM rests clearly on changes revealed by muscle biopsy. The characteristic features include the presence of single or multiple, subsarcolemmal or centrally placed rimmed vacuoles. The vacuoles are lined with granular material that, by

Accepted for publication July 17, 1991.

From the Division of Neuromuscular Disease, Department of Neurology, College of Medicine, The Ohio State University, Columbus.

Reprint requests to Room 463, Means Hall, The Ohio State University, 1654 Upham Dr, Columbus, OH 43210 (Dr Mendell).

mon to both IBM filaments and prion proteins suggest a possible relationship to the human prion disorders.<sup>13-16</sup>

## MATERIALS AND METHODS

### Muscle Specimens

All muscle specimens were embedded in gum tragacanth and frozen on wooden chucks in isopentane cooled in liquid nitrogen immediately on removal. In each case, 8- to 10- $\mu\text{m}$  sections were obtained for a battery of histochemical stains to establish the initial diagnosis. Thereafter, the blocks were stored at -70°C until further use. A diagnosis of IBM was established in 24 samples obtained from three different muscle groups (biceps, n=16; deltoid, n=6; and quadriceps, n=2). All of these biopsy specimens demonstrated common light microscopic features, including rimmed vacuoles, varying degrees of endomysial inflammation, and scattered angular fibers.<sup>4</sup> To be included in the study, an absolute requirement was the presence of typical cytoplasmic or intranuclear filaments fulfilling previously described criteria.<sup>1,2,4</sup> Additional muscle samples studied included polymyositis (n=13) and dermatomyositis (n=19). These patients all fulfilled the criteria of Bohan and Peter.<sup>17</sup> A variety of other myopathies were also examined, including biopsy specimens taken from patients with oculopharyngeal muscular dystrophy (n=4), acid maltase deficiency (n=2), chloroquine myopathy (n=1), distal myopathy (n=1), periodic paralysis (n=1), hereditary vacuolar myopathies of unknown cause (n=5), Duchenne muscular dystrophy (n=2), and phosphoglycerate mutase deficiency (n=1).

### Congo Red Staining

A modification of the previously described alkaline Congo red method<sup>18</sup> provided the most specific staining. Adjustment of the differentiating and Congo red solutions to a pH of 10.5 to 11.0 reduced background staining, especially in comparison with the staining methods for amyloid by Bennhold,<sup>19</sup> Highman,<sup>20</sup> and Lieb.<sup>21</sup>

Fresh-frozen 10- to 12- $\mu\text{m}$  muscle biopsy sections were placed on methanol-cleaned slides. All solutions used for staining were prepared at the time of use and then discarded. Sections were placed in Mayer's hematoxylin<sup>22</sup> for 10 minutes, rinsed in three changes of distilled water, transferred to a solution containing 80% ethanol saturated with sodium chloride, and adjusted to a pH of 10.5 to 11.0 with 1% sodium hydroxide. The sections were then stained for 1 hour with Congo red dye (0.2 g in 100 mL of 80% ethanol saturated with sodium chloride and adjusted to a pH of 10.5 to 11.0 with 1% sodium hydroxide). Following staining, sections were dehydrated in 95% ethanol and absolute ethanol, cleared in xylene, and mounted in a synthetic mounting medium (Permount).

Potassium permanganate method, as described by Wright et al,<sup>23</sup> was used for preincubation in some cases.

### Immune Staining

For antibody localization, 8- to 10- $\mu\text{m}$  sections of fresh-frozen muscle biopsy specimens were fixed in acetone for 1 minute.

Antibody against human transthyretin or human P component (ATAB, Scarborough, Mass) was incubated for 1 hour at room temperature at a 1:50 dilution (matched for protein content with control serum samples). Sections were washed in phosphate-buffered saline and incubated for 1 hour at room temperature with biotinylated anti-sheep IgG (Jackson Immunoresearch) at a 1:200 dilution. Fluorescein-conjugated avidin (EY Labs, San Mateo, Calif) at a 1:200 dilution was used to visualize antibody localization.

### Electron Microscopy

For ultrastructure, muscle specimens were clamped *in situ*, removed, and placed in a solution containing 3% glutaraldehyde in 0.1 mol/L phosphate buffer for 30 minutes. The samples were dissected from the clamp, and 1- to 2-mm cubes were kept in glutaraldehyde for 5 hours, postfixed for 1 hour in 2% osmium tetroxide and 0.1 mol/L phosphate buffer, dehydrated in graded ethanol, and embedded in low-viscosity embedding media. Sections, 1  $\mu\text{m}$  thick, stained with toluidine blue were examined under light microscopy, and appropriate blocks were selected for electron microscopy examination.

### Muscle Fiber Quantitation

The frequency of amyloid-positive fibers was determined in 15 IBM cases selected on the basis of random number assignment. Amyloid-positive fibers and total number of vacuolated fibers were counted in Congo red-stained sections under polarized light. Adjacent fresh-frozen sections of muscle stained with adenosine triphosphate at a pH of 9.4<sup>24</sup> were projected onto a video screen with an overlaid grid to provide orientation. All muscle fibers in the section were counted.

## RESULTS

### Patient Population

Twenty-four consecutive cases of IBM fulfilled the previously described light and electron microscopic criteria.<sup>1,2,4</sup> The clinical features did not differ in any way from the largest population of patients recently described.<sup>1</sup> There were 12 men and 12 women. The mean age at diagnosis was 64.3 years (range, 32 to 76 years), with only three patients aged below 60 years (two men aged 30 and 38 years; one woman aged 57 years). Onset of symptoms prior to diagnosis varied from 1.5 to 15 years. Only one patient had an associated connective tissue disease, rheumatoid arthritis. Other disorders included diabetes mellitus in two patients, colon cancer in one patient, and congenital hypogammaglobulinemia in one patient.

### Congo Red Staining in IBM

The Table shows the results of Congo red staining. All IBM cases demonstrated intracellular Congo red, green-birefringent deposits that were heterogeneous in appearance (Fig 1). The green-

birefringent amyloid deposits varied in size, measuring 1  $\times$  2 to 8  $\mu\text{m}$  and rarely up to 20  $\mu\text{m}$  in length. These deposits assumed different shapes; some were delicate and wispy appearing and others were more plaquelike. Occasional deposits were intranuclear. In bright-field microscopy, the Congo red color appeared as a muted red compared with brighter red extracellular deposits, usually associated with the systemic amyloidoses.

### Congo Red Staining of Control Specimens

Control specimens included cases of dermatomyositis and polymyositis and a variety of vacuolar myopathies (Table). Chloroquine and acid maltase deficiencies are particularly notable for autophagic features that include whorls of membranous material, myelin figures, and secondary lysosomes.<sup>25</sup> None of these cases showed amyloid deposits as seen in IBM. However, in rare autophagic vacuoles (irrespective of the disease) very small (250- to 400-nm) green-birefringent granules were infrequently seen within the vacuoles. These differed from IBM deposits because of their smaller punctate appearance.

Five cases of hereditary vacuolar myopathies were evaluated. Four of these cases were similar to those in the family described by Kalimo et al,<sup>26</sup> while the other was a case of vacuolar myopathy of skeletal and cardiac muscle. In a single muscle fiber, of more than 100 vacuolated fibers examined in these five cases, a linear, green-birefringent deposit similar to that observed in IBM was seen. The nature of this deposit remains unknown and electron microscopy of the specimens in these cases showed only autophagic vacuoles, but no filaments typical of IBM.

In addition, in a case of distal myopathy (showing rimmed vacuoles but no inflammation), congophilic, green-birefringent deposits were seen in the cytoplasm and the muscle also showed 15- to 18-nm filaments adjacent to vacuoles, identical to those seen in IBM. Similar filaments, appearing in distal myopathy, have previously been described.<sup>27</sup>

### Quantitation of Amyloid-Positive Fibers

In IBM, the amyloid deposits were restricted to vacuolated fibers and showed no relation to the inflammatory infiltrate typical of IBM. The deposits were usually seen adjacent to vacuoles, and less often perinuclear. Intranuclear amyloid deposits were seen rarely. The number of amyloid-positive fibers varied greatly between cases, but quantitative morphologic studies demonstrated a linear correlation with the number of

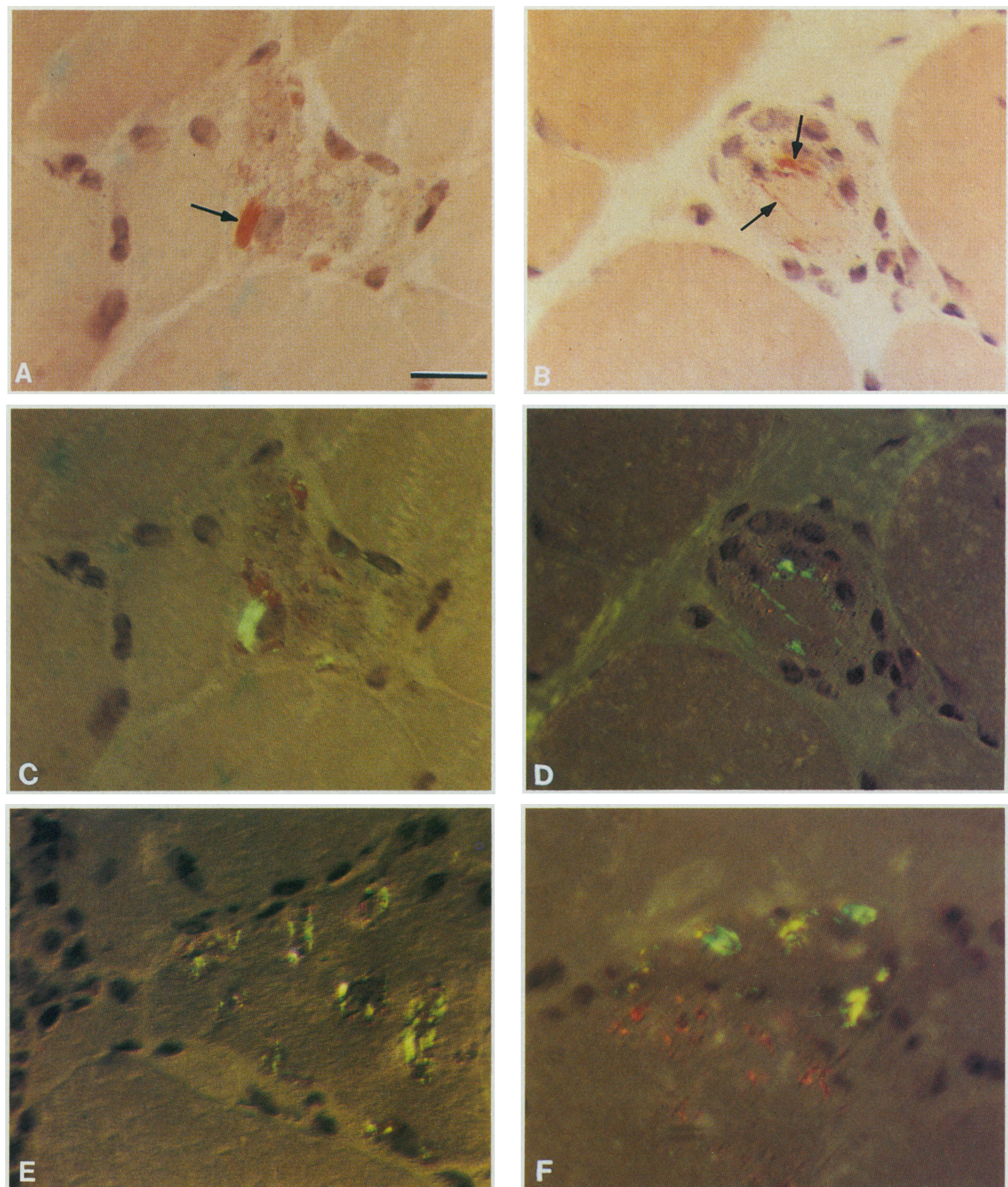


Fig 1.—Vacuolated fibers in inclusion body myositis show Congo red (arrows in A and B) and corresponding green-birefringent intracellular amyloid deposits (C and D), respectively. Delicate wispy deposits (E) contrast to the plaquelike deposits (F) (bar in A = 20  $\mu\text{m}$ ).

vacuolated fibers per biopsy ( $r^2$  value for linear regression line is .892; five of 15 data points lie within 90% confidence level) (Fig 2).

#### Immune and Histochemical Staining

Amyloid deposits in IBM retained their affinity for Congo red dye after incubation with potassium permanganate.

This finding distinguishes the IBM amyloid fibril proteins from those observed in reactive (AA type) amyloidosis.<sup>28</sup> The IBM muscle specimens

Amyloid Deposits in Myopathies			
Diagnosis	No.	Congo Red Deposits	
		Present	Absent
Inclusion body myositis	24	24	0
Polymyositis	13	0	13
Dermatomyositis	19	0	19
Duchenne dystrophy	2	0	2
Chloroquine	1	0	1
Periodic paralysis	1	0	1
Acid maltase deficiency	2	0	2
Phosphoglycerate mutase deficiency	1	0	1
Oculopharyngeal muscular dystrophy	4	0	4
Hereditary vacuolar myopathy	5	1	4
Distal myopathy	1	1	0

showed no immune staining with anti-sera to human P component, transthyretin, or immunoglobulin light chains.

#### Electron Microscopy

The IBM filaments observed in all of our cases ranged in size from 15 to 20 nm with the majority measuring approximately 16 nm ( $16.6 \pm 2.3$  [mean  $\pm$  SD], based on 25 random measurements). The maximum length of individual IBM filaments observed was 0.8  $\mu\text{m}$ . To compare IBM filaments with those of systemic amyloidosis, we studied cardiac muscle laden with transthyretin amyloid deposits. The filaments appeared similar, but in cardiac amyloid the diameter was 8 to 13 nm (mean  $\pm$  SD,  $10.6 \pm 1.77$  nm) compared with IBM filaments measuring 15 to 18 nm (mean  $\pm$  SD,  $16.6 \pm 2.3$  nm) (Fig 3).

#### COMMENT

In this study, we found Congo red, green-birefringent deposits especially in vacuolated muscle fibers in IBM. These deposits are amyloid by definition because of their affinity for Congo red dye and the characteristic green birefringence demonstrated on polarization microscopy.<sup>11,12</sup> The amyloid deposits in IBM were heterogeneous, some delicate and wispy, and others more plaque-like in appearance. These intracellular collections of amyloid occurred adjacent to vacuoles, less often perinuclear, and rarely intranuclear. The distribution corresponds to the typical location of the characteristic filaments, which are the hallmark and distinguishing feature of IBM.<sup>14</sup> These findings strongly indicate that the amyloid deposits seen by histochemical staining and IBM filaments are one and the same. This is further substantiated by the striking ultrastructural resemblance of IBM to amyloid filaments.<sup>11,12</sup> In fact, it was the morphologic similarity to amyloid filaments that served as a

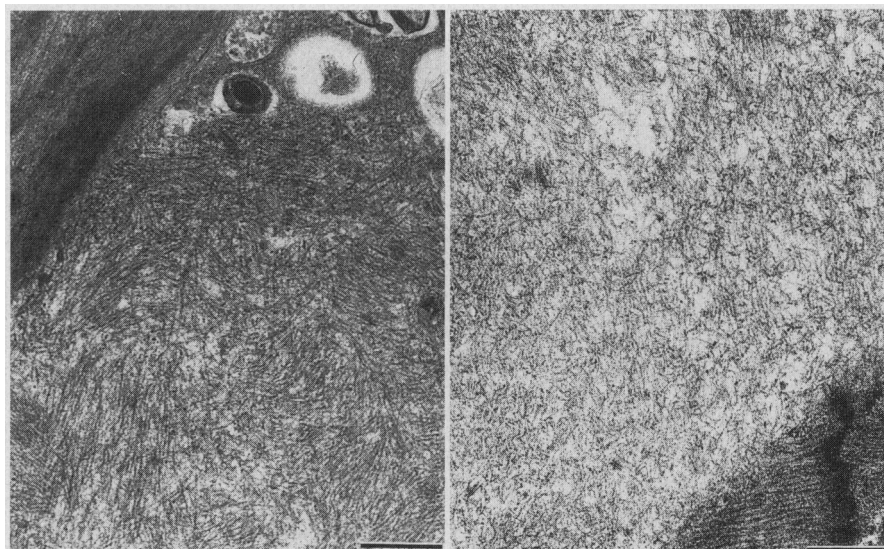


Fig 3.—Electron micrographs comparing amyloid filaments in inclusion body myositis (left) and cardiac amyloid (right). Bar = 0.5  $\mu\text{m}$ .

stimulus for us to examine IBM muscle biopsy specimens using Congo red dye.

Control specimens included other types of inflammatory myopathies and other vacuolar myopathies. No intracellular amyloid deposits were seen in cases of polymyositis or dermatomyositis. This finding has practical implications, indicating that alkaline Congo red staining can facilitate the diagnosis and differentiation of IBM from other inflammatory myopathies. The advantages of Congo red staining are obvious when compared with the effort and expense involved in searching for IBM filaments by electron microscopy. A note of caution, however, is that the number of positive fibers varies greatly between cases (Fig 2) and the  $\times 40$  objective is usually required to see these small intracellular deposits. A wide array of vacuolar myopathies were used as control samples. In one previously diagnosed case of distal myopathy, showing

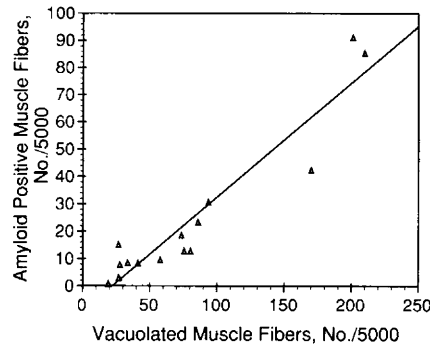


Fig 2.—Graph of linear correlation of the number of amyloid positive fibers compared with the number of vacuolated fibers in 15 randomly selected cases of inclusion body myositis ( $r^2 = .892$ ).

no inflammation, typical green-birefringent deposits were found. This case also exhibited 15- to 18-nm filaments by electron microscopy. These filaments have been found in other cases of distal myopathy,<sup>27</sup> serving to blur the distinction between some types of distal myopathy and IBM. There was one additional case, however, of a hereditary vacuolar myopathy similar to the X-linked autophagic myopathy described by Kalimo et al<sup>28</sup> that showed one positive muscle fiber. Of interest is that muscle biopsy specimens were available from two brothers and two additional cases of hereditary vacuolar myopathies and none showed amyloid deposits. Furthermore, electron microscopy failed to reveal IBM filaments in this case. We do not have an explanation for this single positive fiber of more than 100 vacuolated fibers examined; it most likely represented an artifact. One additional caveat for interpretation was the occasional

appearance of green-birefringent punctate granules found within autophagic vacuoles irrespective of diagnoses (eg, acid maltase deficiency, IBM). The small size and punctate appearance allows them to be differentiated from IBM filaments.

Apart from the practical application of these findings, the most important question relates to the significance of amyloid filaments in IBM. Amyloid proteins are heterogeneous, and the specific protein of origin varies with the disease process. The intracellular location of amyloid deposits in IBM suggests a distinction from the proteins associated with systemic amyloidosis. Further immune staining failed to reveal any cross reactivity with human P component (a nonspecific finding in many types of systemic amyloidosis), transthyretin, or immunoglobulin light chains. The location of IBM-associated amyloid favors a protein synthesized within the cell. However, whether it represents an altered protein derived from a normal gene product or an isoform of a normal protein resulting from a gene mutation cannot be distinguished. For example, recent studies have shown that the 4.2-kd amyloid protein<sup>29-31</sup> of Alzheimer's disease is derived from a much larger amyloid precursor protein encoded by a gene on chromosome 21.<sup>32-35</sup> Antibody studies suggest that accumulations of amyloid precursor in secondary lysosomes lead to proteolytic events that form the 4.2-kd amyloid peptide.<sup>36</sup> The close association of IBM-associated amyloid with autophagic vacuoles also raises the possibility of a posttranslational modification of a normal muscle protein within an acidic degradative vacuolar compartment. Through such posttranslational modification, it is possible that the end product might acquire resistance to proteases and become amyloidogenic.

Another consideration raised by the amyloidogenic properties of IBM filaments relates to the earlier proposal of Chou<sup>8</sup> of an infectious cause for IBM. Although no evidence supports that IBM is related to mumps virus,<sup>9,10</sup> the filaments do share properties with prions, another class of infectious agent.<sup>13-16</sup> Prions have been held accountable for the transmissible central nervous system neurodegenerative disorders, including scrapie of sheep and goats, and the human diseases, ie, kuru, Creutzfeldt-Jakob disease, and Gerstmann-Sträussler syndrome.<sup>13-16,37-39</sup> Prusiner and colleagues<sup>13</sup> demonstrated that purified scrapie prions, isolated from hamster brains, aggregated into rod-shaped particles measuring 10 to 20 nm in diameter, resembled amyloid

by electron microscopy, and showed green birefringence using Congo red dye. Subsequent studies<sup>40-41</sup> showed that infectivity was inseparable from a sialoglycoprotein of molecular weight 27 000 to 30 000, designated PrP 27-30. Antibodies raised to PrP 27-30 neutralized scrapie infectivity.<sup>42</sup> Furthermore, PrP 27-30 antisera not only localized within plaques of scrapie-infected hamster brain but also revealed filaments measuring 16 nm in diameter within the plaques.<sup>14</sup> The diameter of the prion and IBM filaments are virtually identical, and both are slightly larger than systemic amyloid filaments.<sup>43</sup>

Additional similarities between IBM and human prion diseases are worthy of note. Approximately 5% to 15% of cases of Creutzfeldt-Jakob disease are familial, and most cases of Gerstmann-Sträussler syndrome are inherited.<sup>38,39</sup> Of particular interest is that both sporadic and familial forms of IBM occur.<sup>44,45</sup> In fact, of the 24 subjects forming the basis for this report, two were brothers. In addition, the recently reported familial form of IBM affecting five of six male siblings was associated with periventricular leukoencephalopathy.<sup>45</sup> In Gerstmann-Sträussler syndrome and familial Creutzfeldt-Jakob disease, accumulating evidence supports both an infectious and a genetic basis related to PrP encoded by a cellular gene.<sup>46-50</sup> PrP genes have been sequenced in humans,<sup>50</sup> various species of hamsters,<sup>51</sup> mice,<sup>52,53</sup> rats,<sup>54</sup> and sheep.<sup>55</sup> In scrapie disease, the infection appears to be linked to a PrP isoform that differs from control PrP because of a posttranslational modification.<sup>56</sup> In the human prion disease, Gerstmann-Sträussler syndrome, a point mutation of the PrP gene on chromosome 20 has been demonstrated at codon 102.<sup>47,48</sup> The proline to leucine substitution codes for an isoform of PrP that may be responsible for the disease.

Further studies will be required to establish the nature of IBM filaments. The amyloidogenic properties provide new insight and suggest approaches not previously considered for this disease. The relation to human prion diseases is provocative but not by any means established. Identification of a transmissible agent will require approaches paralleling those employed for the studies of transmissible neurodegenerative diseases.<sup>15</sup> Perhaps even more importantly, identifying intracellular amyloid also raises possibilities of altered muscle proteins that accumulate within the cytoplasm because of resistance to the usual intracellular digestive process. Such changes could be acquired or genetic. Of interest is the growing list of neurologic diseases arising from muta-

tions in amyloidogenic proteins.<sup>57</sup> No matter what final explanation accounts for the appearance of amyloid fibrils in IBM, the observations presented here provide clues to the pathogenesis of this poorly understood disorder, which have not previously been brought into focus.

The authors acknowledge the useful discussions with Allen Yates, MD, PhD, and Leopold Liss, MD, of the Department of Pathology, The Ohio State University, Columbus, and the assistance of Nancy Hodges in the preparation of this manuscript.

## References

- Yunis EJ, Samaha FJ. Inclusion body myositis. *Lab Invest*. 1971;25:240-248.
- Carpenter S, Karpati G, Heller I, Eisen A. Inclusion body myositis: a distinct variety of idiopathic inflammatory myopathy. *Neurology*. 1978;28:8-17.
- Ringel SP, Kenny CE, Neville HE, Giorno R, Carry MR. Spectrum of inclusion body myositis. *Arch Neurol*. 1987;44:1154-1157.
- Lotz BP, Engel AG, Nishino H, Stevens JC, Litchy WJ. Inclusion body myositis: observations in 40 patients. *Brain*. 1989;112:727-747.
- Riggs JE, Schuchet SS, Gutmann L, Lerfeld SC. Childhood onset inclusion body myositis mimicking limb-girdle muscular dystrophy. *J Child Neurol*. 1989;4:283-285.
- Arahata K, Engel AG. Monoclonal antibody analysis of mononuclear cells in myopathies, I: quantitation of subsets according to diagnosis and sites of accumulation and demonstration and counts of muscle fibers invaded by T cells. *Ann Neurol*. 1984;16:193-208.
- Chou S-M. Myxovirus-like structures in a case of human chronic polyomyositis. *Science*. 1967;158:1453-1455.
- Chou S-M. Inclusion body myositis: a chronic persistent mumps myositis? *Hum Pathol*. 1986;17:765-777.
- Ramamohan KW, Wolinsky J, Omerza J, Gales T, Kissel JT, Mendell JR. Mumps virus in IBM: studies implicating cross-reactivity accounting for antigen localization. *Neurology*. 1988;38(suppl 1):151.
- Nishino H, Engel AG, Rima BK. The mumps hypothesis of inclusion body myositis. *Ann Neurol*. 1989;25:260-264.
- Glenner GG. Amyloid deposits and amyloidosis, I: the β-fibrillloses. *N Engl J Med*. 1980;302:1283-1292.
- Glenner GG. Amyloid deposits and amyloidosis, II: the β-fibrillloses. *N Engl J Med*. 1980;302:1333-1343.
- Prusiner SB, McKinley MP, Bowman KA, et al. Scrapie prions aggregate to form amyloid-like birefringent rods. *Cell*. 1983;35:349-358.
- DeArmond SJ, McKinley MP, Barry RA, Braunfeld MB, McCollough JR, Prusiner SB. Identification of prion amyloid filaments in scrapie-infected brain. *Cell*. 1985;41:221-235.
- Prusiner SB. Prions and neurodegenerative diseases. *N Engl J Med*. 1987;317:1571-1581.
- Prusiner SB. Scrapie prions. *Ann Rev Microbiol*. 1989;43:345-374.
- Bohan A, Peter JP. Polymyositis and dermatomyositis. *N Engl J Med*. 1975;292:344-347.
- Puchtler H, Sweat F, Levine M. On the binding of Congo red by amyloid. *J Histochem Cytochem*. 1962;10:355-364.
- Mallory FB. *Pathological Technique*. New York, NY: Hafner Publishing Co; 1961:133-134.
- Highman B. Improved methods for demonstrating amyloid in paraffin sections. *Arch Pathol*. 1946;41:559-562.
- Lieb E. Permanent stain for amyloid. *Am J Clin Pathol*. 1947;17:413-414.
- Luna LG. *Manual of Histologic Staining*.

23. Wright JR, Calkins E, Humphrey RL. Potassium permanganate reaction in amyloidosis: a histologic method to assist in differentiating forms of this disease. *Lab Invest*. 1977;36:274-281.
24. Dubowitz V, Brooke MH. *Muscle Biopsy: a Modern Approach*. Philadelphia, Pa: WB Saunders Co; 1973:32.
25. Engel AG. Vacuolar myopathies: multiple etiologies and sequential structural studies. In: Pearson CM, Mostofi FK, eds. *The Striated Muscle*. Baltimore, Md: Williams & Wilkins; 1973:301-341.
26. Kalimo H, Savontaus M-L, Lang H, et al. X-linked myopathy with excessive autophagy: a new hereditary muscle disease. *Ann Neurol*. 1988; 23:258-265.
27. Matsubara S, Tanabe H. Hereditary distal myopathy with filamentous inclusions. *Acta Neurol Scand*. 1982;65:363-368.
28. Kitamoto T, Tateishi J, Hikita K, Nagara H, Takeshita I. A new method to classify amyloid fibril proteins. *Acta Neuropathol*. 1985;67:272-278.
29. Selkoe DJ. Biochemistry of altered brain proteins in Alzheimer's disease. *Ann Rev Neurosci*. 1989;12:463-490.
30. Glenner GG, Wong CW. Alzheimer's disease: initial report of the purification and characterization of a novel cerebrovascular amyloid protein. *Biochem Biophys Res Commun*. 1984;120:885-890.
31. Glenner GG, Wong CW. Alzheimer's disease and Down's syndrome: sharing of a unique cerebrovascular amyloid protein. *Biochem Biophys Res Commun*. 1984;122:1131-1135.
32. Allsop D, Wong CW, Ikeda S-I, Landon M, Kidd M, Glenner G. Immunohistochemical evidence for the derivation of a peptide ligand from the amyloid  $\beta$ -protein precursor of Alzheimer's disease. *Proc Natl Acad Sci U S A*. 1988;85:2790-2794.
33. Goldgaber D, Lerman MI, McBride W, Safiotti U, Gajdusek DC. Characterization and chromosomal localization of a cDNA encoding brain amyloid of Alzheimer's disease. *Science*. 1987;235:877-880.
34. Masters CL, Simms G, Weinman NA, Multhaup G, McDonald BL, Beyreuther K. Amyloid plaque core protein in Alzheimer's disease and Down syndrome. *Proc Natl Acad Sci U S A*. 1985;82:4245-4249.
35. Tanzi RE, Gusella JF, Watkins PC, et al. Amyloid  $\beta$ -protein gene: cDNA, mRNA distribution and genetic linkage near the Alzheimer locus. *Science*. 1987;235:880-884.
36. Benowitz LI, Rodriguez W, Paskevich P, Mufson EJ, Schenk D, Neve RL. The amyloid precursor protein is concentrated in neuronal lysosomes in normal and Alzheimer disease subjects. *Exp Neurol*. 1989;106:237-250.
37. Kitamoto T, Tateishi J, Tashima T, et al. Amyloid plaques in Creutzfeldt-Jakob disease stain with prion protein antibodies. *Ann Neurol*. 1986;20:204-208.
38. Masters CL, Gajdusek DC, Gibbs CJ Jr. The familial occurrence of Creutzfeldt-Jakob disease and Alzheimer's disease. *Brain*. 1981;104:535-558.
39. Masters CL, Gajdusek DC, Gibbs CJ Jr. Creutzfeldt-Jakob disease virus isolations from the Gerstmann-Sträussler syndrome. *Brain*. 1981; 104:559-588.
40. Bolton DC, McKinley MP, Prusiner SB. Identification of a protein that purifies with the scrapie prion. *Science*. 1982;218:1309-1311.
41. Bolton DC, Meyer RK, Prusiner SB. Scrapie PrP 27-30 is a sialoglycoprotein. *J Virol*. 1985;53:596-606.
42. Gabizon R, McKinley MP, Groth DF, Prusiner SB. Immunoaffinity purification and neutralization of scrapie prion infectivity. *Proc Natl Acad Sci U S A*. 1988;85:6617-6621.
43. Cohen AS, Shirahama T, Skinner M. Electron microscopy of amyloid. In: Ham JR, ed. *Electron Microscopy of Proteins*. Orlando, Fla: Academic Press Inc; 1982;3:165-206.
44. Baumbach LL, Neville HE, Ringel SP, Garcia C, Sujansky E. Familial inclusion body myositis: evidence for autosomal dominant inheritance. *Ann Hum Genet*. 1990;47(suppl):A48.
45. Cole AJ, Kuzniecky R, Karpati G, Carpenter S, Andermann E, Andermann F. Familial myopathy with changes resembling inclusion body myositis and periventricular leucoencephalopathy. *Brain*. 1988;111:1025-1037.
46. Ridley RM, Baker HF, Crow TJ. Transmissible and nontransmissible neurodegenerative disease: similarities in age of onset and genetics in relation to aetiology. *Psychol Med*. 1986;16:199-207.
47. Hsiao K, Baker HF, Crow TJ, et al. Linkage of a prion protein missense variant to Gerstmann-Sträussler syndrome. *Nature*. 1989;338:342-345.
48. Hsiao KK, Westaway DA, Prusiner SB. An amino acid substitution in the prion protein of ataxic Gerstmann-Sträussler syndrome. *Am J Hum Genet*. 1988;43:A87.
49. Westaway D, Carlson GA, Prusiner SB. Unraveling prion diseases through molecular genetics. *Trends Neurosci*. 1989;12:221-227.
50. Kretzschmar HA, Stowring LE, Westaway D, Stubblebine WH, Prusiner SB, DeArmond SJ. Molecular cloning of a human prion protein cDNA. *DNA*. 1986;5:315-324.
51. Lowenstein DH, Butler D, McKinley MP, Prusiner SB. Chinese and Armenian hamster prion protein genes. *J Cell Biol*. 1988;107:136. Abstract.
52. Locht C, Chesebro B, Race R, Keith JM. Molecular cloning and complete sequence of prion protein cDNA from mouse brain infected with the scrapie agent. *Proc Natl Acad Sci U S A*. 1986; 83:6372-6376.
53. Westaway D, Goodman P, Mirenda C, et al. Distinct prion proteins in short and long scrapie incubation period mice. *Cell*. 1987;51:651-652.
54. Liao Y-C, Tokes Z, Lim E, et al. Cloning of rat 'prion-related protein' cDNA. *Lab Invest*. 1987;57:370-374.
55. Goldman W, Hunter N, Multhaup G, et al. The PrP gene in natural scrapie. *Alzheimer Dis Assoc Disord*. 1988;2(suppl):331. Abstract.
56. Basler K, Oesch B, Scott M, et al. Scrapie and cellular PrP isoforms are encoded by the same chromosomal gene. *Cell*. 1986;46:417-428.
57. Wright AF, Goedert M, Hastie ND. Beta amyloid resurrected. *Nature*. 1991;349:653-654.